HIGH-GRADIENT TESTS ON *S*-BAND 2M-LONG ACCELERATING STRUCTURES FOR KEKB INJECTOR LINAC

Y. Igarashi†, The Graduate University for Advanced Studies (SOKENDAI)
S. Yamaguchi, Y. Higashi, A. Enomoto, T. Oogoe, K. Kakihara, and S. Ohsawa, KEK
1-1 Oho, Tsukuba, Ibaraki, 305-0801 Japan
H. Tomizawa, T. Taniuchi, H. Hanaki, Spring-8
1-1-1 Kouto, Mikazuki-cho, Sayo-gun, Hyogo 679-5198, Japan

Abstract

In this paper, we describe high-gradient test results performed on *S*-band 2m-long accelerating structures for KEKB injector linac. High-gradient tests were performed on three types of accelerating structures: (1) a conventional accelerating structure for KEKB injector linac, (2) an accelerating structure whose input and output couplers were replaced by ones without a crescent-shaped cut, and (3) a conventional accelerating structure which was rinsed with high-pressure ultrapure water. As a result of the tests, an average accelerating gradient of more than 40 MV/m was obtained in all structures. Especially, 45 MV/m was achieved in a structure rinsed with high-pressure ultrapure water with a short rf processing time and a low breakdown rate (this gradient was limited by the klystron output power). Black patterns were observed at a crescent-shaped cut and the iris of the coupler cells. The simulated surface current densities were higher by about 10 times than that of the other surfaces of the cells. The measured momentum spectra were reproduced qualitatively by a simulation. It was found that the breakdown rate decreased significantly after conditioning.

1 HIGH-GRADIENT TEST OF THE ACCELERATING STRUCTURE

1.1 Tested structures

The 2m-long accelerating structure for KEKB injector linac is of a quasi-constant gradient type and has 54 regular cells with 2 coupler cells (Fig. 1). It is operated in the $2\pi/3$ mode at 2856 MHz. This structure is fabricated using a high-precision turning lathe with a diamond byte and a electroplating fabrication method. There is a crescent-shaped cut at the opposite side of the waveguide iris to correct for any asymmetry of the electromagnetic fields in coupler cell. High-gradient tests were performed on three types of accelerating structures:

Type (1): The conventional accelerating structure for KEKB injector linac [1].

Type (2): The accelerating structure whose input and output couplers were replaced with those without a crescent-shaped cut. After a high-gradient test of Type (1), a black pattern was observed at the crescent-shaped cut of the output coupler cell.

Type (3): The conventional accelerating structure which was rinsed with high-pressure ultrapure water. The high-pressure ultrapure water rinsing technique (HPR) is very effective to improve the field gradients for normal conducting and superconducting rf cavities. HPR eliminates surface contamination, such as dust particles, that is thought to be one of the causes of field emission. We applied this technique to the 2m-long accelerating structure (Fig. 2). It was observed in preliminary tests that HPR could reduce dust particles to 1/10 or less on a disk surface[1].

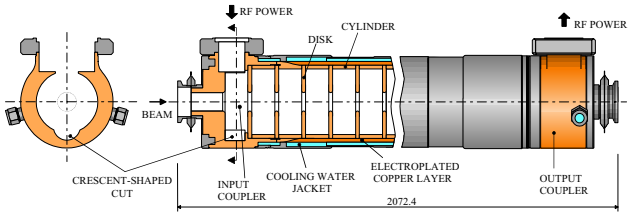

Fig. 1: Schematic of the 2m-long accelerating structure for KEKB injector linac.

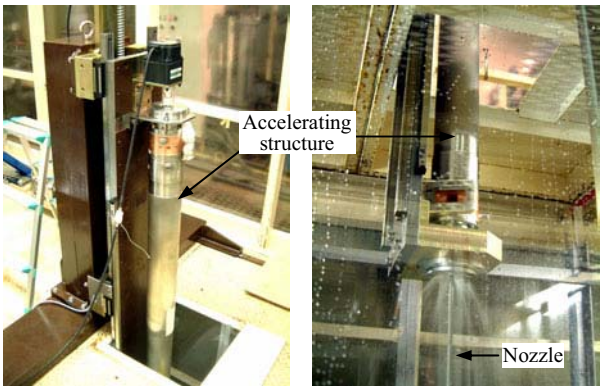

Fig. 2: High-pressure ultrapure water rinsing of the 2m-long accelerating structure.

1.2 Experimental results

The pulse width and repetition rate of the rf pulse were 4.0 μsec and 50 Hz, respectively. At first, a test was carried out with the SLED detuned; next, it was carried out with the SLED tuned. Reflection of the rf power from the accelerating structure or waveguides, and the vacuum pressure of the ion pumps were used as an interlock. The total amount of dark current caused by the field-emitted electrons was measured by two Faraday cups set upstream and downstream of the accelerating structure. The vacu-

†yasuhito.igarashi@kek.jp

um pressure of the accelerating structure was maintained at around 1×10^{-6} Pa during rf conditioning.

Table 1 summarizes the high-gradient test results. The average accelerating field *vs*. the number of shots is shown in Fig. 3. The field enhancement factor (β) can be obtained from a modified Fowler-Nordheim (F.N.) plot. F.N. plots are shown in Fig. 4, and the β values are shown in Fig. 5 (only Type (3)). As a result of the tests, an average accelerating gradient of 45 MV/m was achieved.

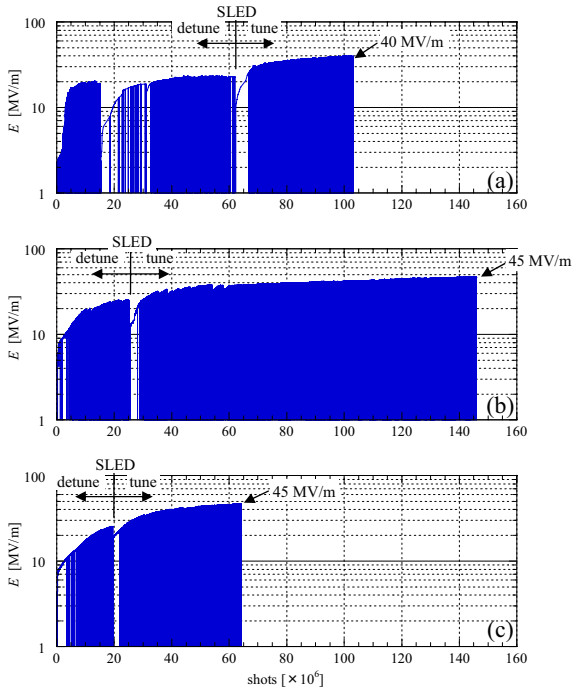

Fig. 3: Average field *vs*. number of shots.
(a) Type(1), (b) Type(2), (c) Type(3).

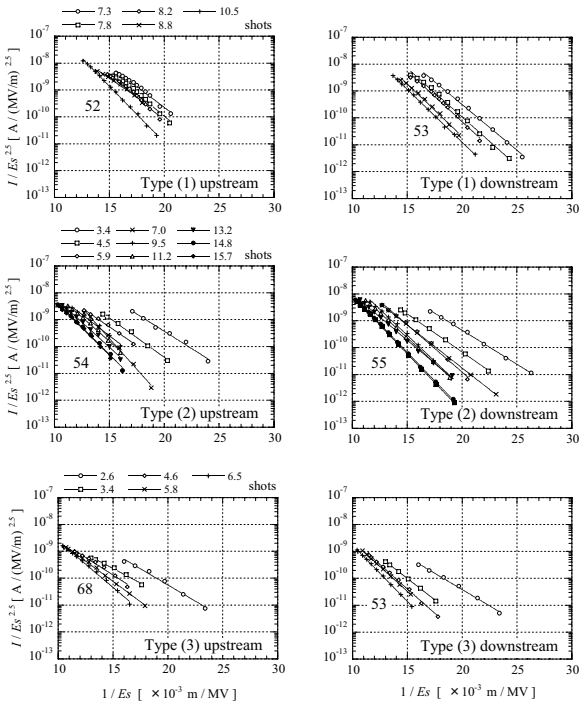

Fig. 4: Modified F. N. plot (SLED tune).

Especially, a structure rinsed with high-pressure ultra-pure water reached 45 MV/m with a short rf process-ing time, low breakdown rate and low dark currents compared with the others. Although this gradient was limited by the klystron output power, we are expecting that more than 45 MV/m can be achieved.

Table 1: Test results of three types of structures.

Type	Time [hour]	Shot [$\times10^7$]	Maximum average field [MV/m]	Peak dark current [μA] up	Peak dark current [μA] down	β up	β down
(1)	542	10.0	40*	570	630	52	53
(2)	812	15.0	45	720	1130	54	55
(3)	356	6.4	45	300	237	68	53

*: Terminated due to a time limit

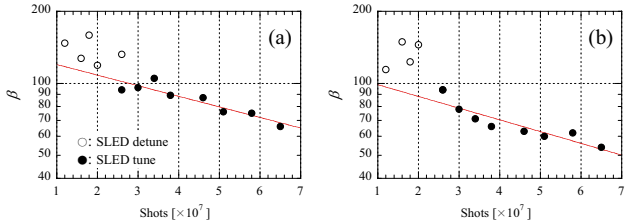

Fig. 5: Field enhancement factor (β) *vs*. number of shots.(Type (3)). (a) upstream, (b) downstream.

2 BLACK PATTERNS INSIDE THE COUPLER CELLS

When we confirmed that inside of the conventional accelerating structure after the high-gradient test, a black pattern was observed at the crescent-shaped cut of the output coupler cell. Also, when we cut the accelerating structure used for the accelerator operation, in order to confirm inside of the input coupler cell, a black pattern was observed at the coupler iris.

We performed simulations of the surface electric field strength and the surface current density on the coupler cell using HFSS. The surface current densities on the crescent-shaped cut and on the coupler iris are shown in Figs. 6 and 7, respectively. From these results, the surface current densities at the location of black patterns were higher by about 10 times than that of the other surfaces of the cells.

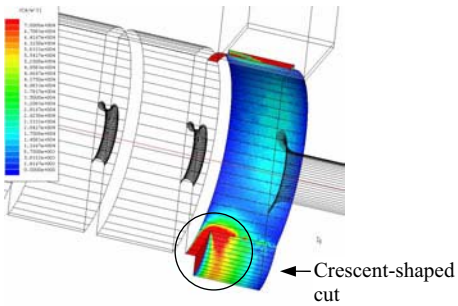

Fig. 6: Simulated surface current density on the crescent-shaped cut.

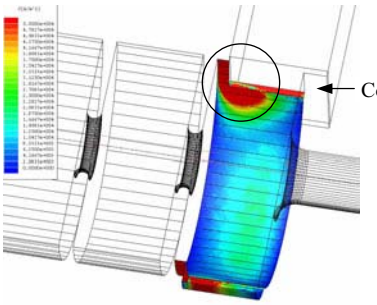

Fig. 7: Simulated surface current density on the coupler iris.

3 MOMENTUM SPECTRA OF DARK CURRENTS

The momentum spectra of the dark currents were measured by a bending magnet with a Faraday cup. The slit aperture was 20 mm. The measured result of Type (3) for an average accelerating gradient of 42 MV/m after 5.7 $\times 10^7$shots is shown in Fig. 8 (dotted line). The dashed line is the simulated momentum spectrum. The simulations were calculated by the ETS code (The simulated structures were constant-impedance types) [2]. An example of the simulated trajectories of the field-emitted electrons is shown in Fig. 9. (In this example, the number of primary electrons is 200. In the actual calculation, it was set to 720,000.) In Fig. 8, the measured momentum spectrum has a slope at the low-energy region, but the simulated momentum spectrum does not have a slope. The phase-space distribution of the field-emitted electrons that arrived at the end of structure was calculated. Fig. 10 show the relation with the momentum and the position x and the angle x'. Most of the electrons are within the aperture size (a = 11.875 mm), and the low-energy electrons have a large angle. The momentum spectrum, recalculated by the electrons with $x < a$ mm and $x' < 0.02$ rad, is shown in Fig.8 (solid line). The electrons with $x' < 0.02$ rad are captured at the cavity disks (collimator) and the slit. The simulation results were qualitatively consistent with the measurement results.

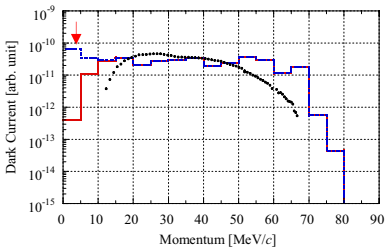

Fig. 8: Momentum spectra of the dark current.

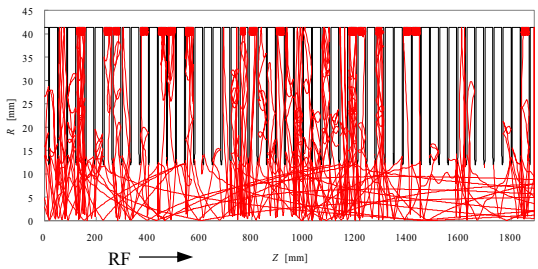

Fig. 9: Example of the field-emitted electrons trajectories.

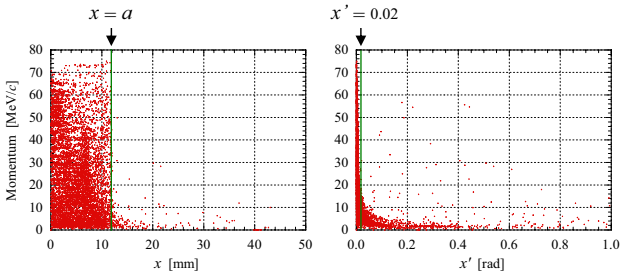

Fig. 10: Momentum *vs.* the position x and the angle x' of the field-emitted electrons that arrived at the end of the structure.

4 RELATION WITH THE AVERAGE ACCELERATING GRADIENT AND THE BREAKDOWN RATE

At the end of high-gradient tests, we examined the relation between the breakdown rate and the average accelerating gradient. The test result of Type (2) is shown in Fig. 11. The breakdown rate was significantly decreased after conditioning.

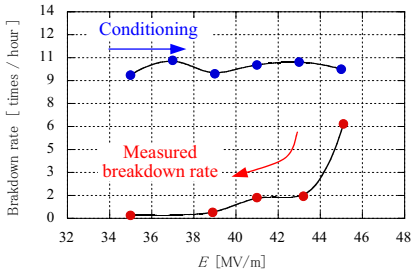

Fig. 11: Relation between the breakdown rate and the average accelerating gradient.

5 SUMMARY

An average accelerating gradient of 45 MV/m was obtained in a structure rinsed with high-pressure ultrapure water with a short rf processing time, a low breakdown rate and low dark currents. Black patterns were observed at a crescent-shaped cut and the iris of the coupler cells. As a result of simulations, the surface current densities were found to be higher by about 10 times than that of the other surfaces of the cells. The measured momentum spectra were qualitatively reproduced by the simulation. It was found that the breakdown rate decreased significantly after conditioning.

6 REFERENCES

[1] Y. Igarashi, et al., "High-gradient Tests on an *S*-band Accelerating Structure", Proc. of the 21st International Linac Conference, LINAC2002, Korea, 2002.

[2] S. Yamaguchi, "Simulation Studies on High-Gradient Experiments", LAL/RT 92-18, 1992.